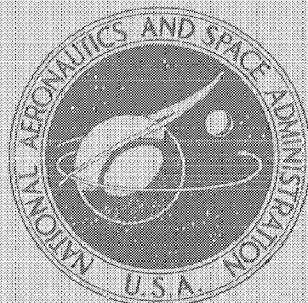


NASA TECHNICAL
MEMORANDUM



NASA TM X-1946

NASA TM X-1946

CASE FILE
COPY

TECHNIQUE FOR INDUCING CONTROLLED
STEADY-STATE AND DYNAMIC INLET
PRESSURE DISTURBANCES
FOR JET ENGINE TESTS

by Carl L. Meyer, John E. McAulay, and Thomas J. Biesiadny

Lewis Research Center

Cleveland, Ohio

1. Report No. NASA TM X-1946	2. Government Accession No.	3. Recipient's Catalog No.	
4. Title and Subtitle TECHNIQUE FOR INDUCING CONTROLLED STEADY-STATE AND DYNAMIC INLET PRESSURE DISTURBANCES FOR JET ENGINE TESTS		5. Report Date January 1970	
		6. Performing Organization Code	
7. Author(s) Carl L. Meyer, John E. McAulay, and Thomas J. Biesiadny		8. Performing Organization Report No. E-5318	
9. Performing Organization Name and Address Lewis Research Center National Aeronautics and Space Administration Cleveland, Ohio 44135		10. Work Unit No. 720-03	
		11. Contract or Grant No.	
		13. Type of Report and Period Covered Technical Memorandum	
12. Sponsoring Agency Name and Address National Aeronautics and Space Administration Washington, D. C. 20546		14. Sponsoring Agency Code	
15. Supplementary Notes			
16. Abstract Capabilities and limitations of a technique for inducing variable-amplitude steady-state or dynamic pressure distortions or dynamic uniform pressure oscillations for jet engine tests are illustrated. In the technique, secondary air was injected through an array of small nozzles uniformly distributed in an engine inlet duct to achieve momentum interchange with the primary air. Secondary-air distribution and flow rate were controlled.			
17. Key Words (Suggested by Author(s)) Test technique Jet engines Inlet pressure disturbances Steady state or dynamic Variable amplitude		18. Distribution Statement Unclassified - unlimited	
19. Security Classif. (of this report) Unclassified	20. Security Classif. (of this page) Unclassified	21. No. of Pages 33	22. Price* \$3.00

*For sale by the Clearinghouse for Federal Scientific and Technical Information
Springfield, Virginia 22151

TECHNIQUE FOR INDUCING CONTROLLED STEADY-STATE AND DYNAMIC INLET PRESSURE DISTURBANCES FOR JET ENGINE TESTS

by Carl L. Meyer, John E. McAulay, and Thomas J. Biesiadny

Lewis Research Center

SUMMARY

An investigation was conducted to evaluate a technique wherein secondary air was injected through an array of small nozzles uniformly distributed in an engine inlet duct to achieve momentum interchange with the primary air forward of the compressor face location. High-response servo-operated valves provided steady-state and dynamic control of secondary airflow.

Through control of secondary-air distribution and flow rate, the technique provides a way of inducing variable-amplitude steady-state or dynamic pressure distortions or dynamic uniform pressure oscillations without excessive random pressure amplitude. Dynamic pressure distortions were not evaluated in this investigation. The amplitude of induced dynamic pressure oscillations attenuated appreciably at frequencies above 20 hertz. Work is currently in progress with the purpose of improving amplitude capabilities at the higher frequencies.

INTRODUCTION

A program to study the influence of steady-state and dynamic compressor-inlet pressure disturbances on engine compressor-system characteristics and operating limits is being conducted at Lewis. For this program, it was necessary to devise experimental techniques for inducing the compressor-inlet disturbances. Screens, for example, are widely used to induce steady-state pressure distortions, but varied screen solidity is required to vary amplitude of the distortion. Rotating devices have been used to induce dynamic uniform pressure disturbances at discrete frequencies (ref. 1), but sufficient amplitude and good waveform are difficult to obtain. Choked stations followed by supersonic flow and shocks have been used to induce dynamic random pressure disturbances (ref. 2), but good control is difficult to obtain. These techniques thus have application with limitations.

In another technique, secondary air is injected through an array of small nozzles in the engine inlet duct to achieve momentum interchange with the primary air forward of the compressor face. Through control of the secondary-air distribution and flow rate, variable-amplitude steady-state or dynamic pressure distortions or dynamic uniform pressure oscillations can be produced. The secondary nozzles are uniformly distributed circumferentially and radially in a plane normal to the duct centerline. When the secondary air is injected counter to the primary airflow, the momentum interchange upstream of the jet array results in a total pressure loss which may be controlled by varying secondary airflow. Essentially, the converse will be the case when the secondary air is injected in the same direction as the primary flow. (Choice of secondary-flow direction is primarily dependent on the flow uniformity that can be achieved at the compressor-inlet location.)

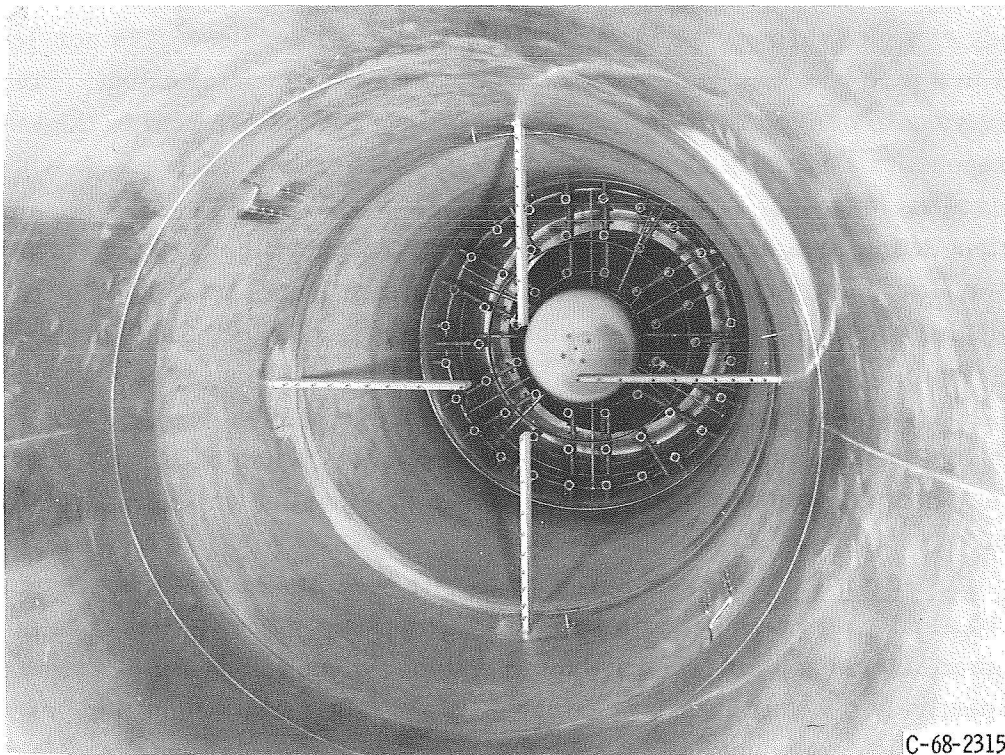
A one-dimensional analysis of the steady-state momentum interchange was made to evaluate potential of the technique and to estimate secondary airflow requirements. Secondary air from a relatively high-pressure source is required to achieve the flow rates with minimum hardware dimensions and blockage in the inlet duct. A system was designed and fabricated for use of secondary air available at nominal pressures up to 10 atmospheres. High-response servo-operated valves of special design for the application were fabricated to provide both dynamic and steady-state control of secondary airflow. The particular system was designed for use with engines of the TF-30 size and flow rates.

This report includes a description and an evaluation of the secondary-air jet system. The evaluation was made primarily while using a duct rather than an engine, but some system evaluation data are included from an engine program. Information is presented which guided the selection of secondary-air injection-plane axial location and flow direction in the inlet duct on the basis of total-pressure uniformity. Analysis and experiment are compared for the selected secondary airflow direction. The capabilities of the secondary-air jet system for inducing variable-amplitude steady-state circumferential and radial pressure distortions are illustrated. The capabilities and limitations of the system for inducing dynamic uniform pressure oscillations of varied discrete frequencies are illustrated. Some potential system modifications are considered, and additional potential system capabilities are described.

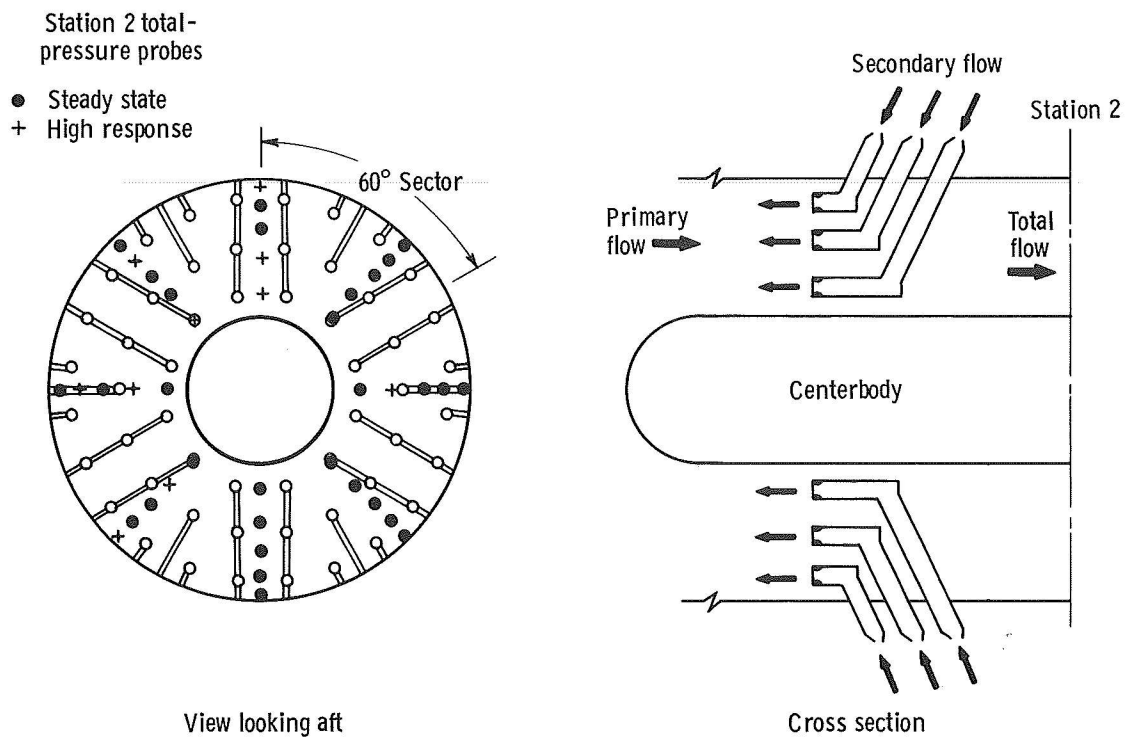
APPARATUS

Secondary-Air Jet System

Jet array. - Fifty-four small secondary-flow nozzles were uniformly distributed circumferentially and radially in an annular axial plane of the inlet duct (fig. 1). A



(a) Jet array and station 1 instrumentation.



(b) Schematic drawing of jet array and station 2 instrumentation.

Figure 1. - Secondary-air jet array and instrumentation in inlet duct.

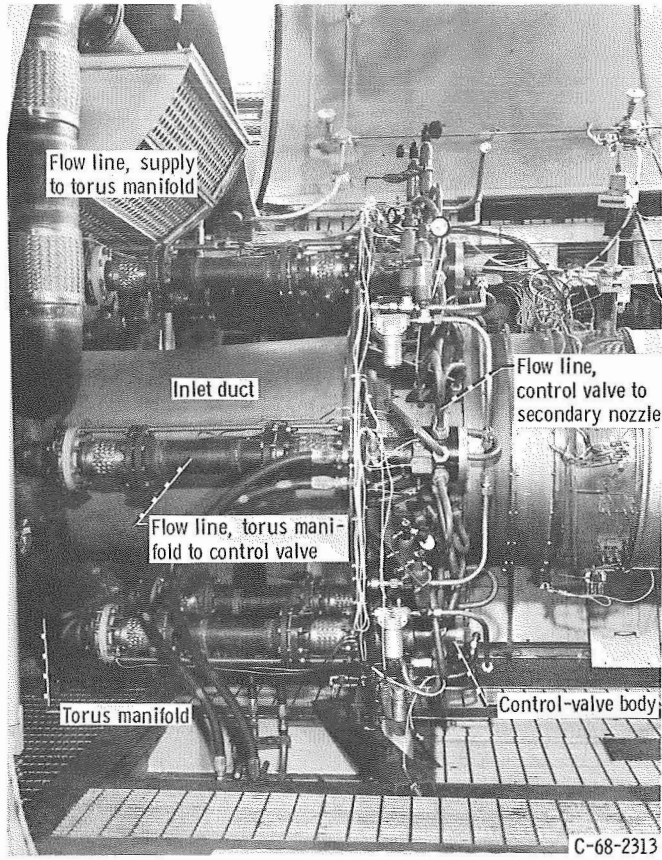
centerbody extended through the plane of discharge of the nozzles. The nozzles were arranged in a pattern which repeated every 60° of circumferential extent. Six flow-control valves, to be discussed subsequently, were provided external to the inlet duct to control secondary airflow to each 60° sector. Separate flow lines were provided from each control valve to each of the nine nozzles in the sector. These flow lines were all of equal length and constant cross-sectional area throughout their length. The radial extents of the flow lines within the inlet duct were formed from flattened tubes to reduce frontal blockage area. Round tubes extended axially from the flattened tubes to the nozzles. Externally, round tubes extended from the control valves to the flattened tubes.

The jet array was mounted in a spool-piece section of inlet ducting. This section and other sections of inlet ducting were interchangeable, which provided a means of inserting the jet array and selecting the injection-plane location and flow direction in the inlet duct.

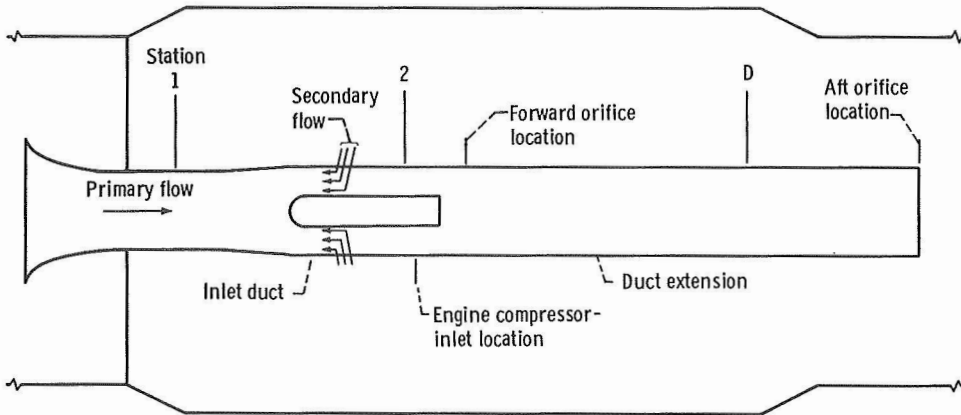
Secondary-air supply system. - Secondary air was available at pressures up to a nominal 10 atmospheres. The main secondary-flow supply line, external to the facility test chamber, included gate-type and butterfly-type valves for on-off and pressure control, respectively. Within the test chamber (fig. 2), the main supply line branched so that secondary flow was supplied by means of two flow lines to a torus manifold around the primary-air inlet duct. For the present investigation, the location of the torus manifold remained fixed. Separate flow lines were provided from the torus manifold to each flow-control valve location and, thus, for each 60° sector of secondary nozzles. The length of these flow lines (which, for dynamic testing, should be as short as possible) was varied when selecting the secondary-air injection-plane location and flow direction in the inlet duct.

Flow-control valves. - Six high-response servo-operated valves of special NASA design for this application provided steady-state and dynamic control of secondary airflow to each 60° sector of secondary nozzles. The valves were designed for operation over an oscillatory frequency range from 0 to a nominal 200 hertz. The valve design provided for control of valve-port area through control of the position of an open-ended piston (fig. 3). Valve ports of $1/4$ -inch (0.635-cm) axial width in the piston and fixed cylinder walls permitted $\pm 1/8$ inch (± 0.318 cm) of piston travel to achieve the range from full-open to full-closed ports. Nine ports were equally spaced circumferentially in each of four axially spaced rows for each piston and cylinder. The midposition about which the piston oscillated and the amplitude of piston travel could be selected within mechanical limits.

The piston-cylinder assembly was inserted into a valve body which provided a valve-discharge circumferential plenum. The inlets to nine secondary airflow lines, for a 60° sector of secondary nozzles, were equally spaced circumferentially around each valve discharge plenum.

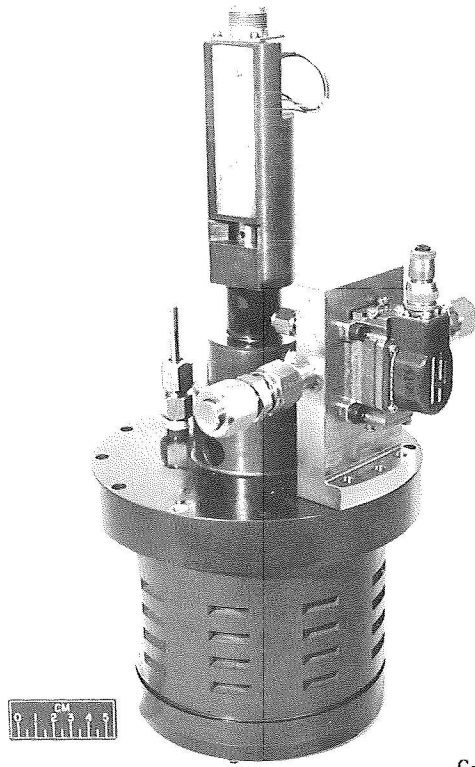


(a) Secondary-air supply system.



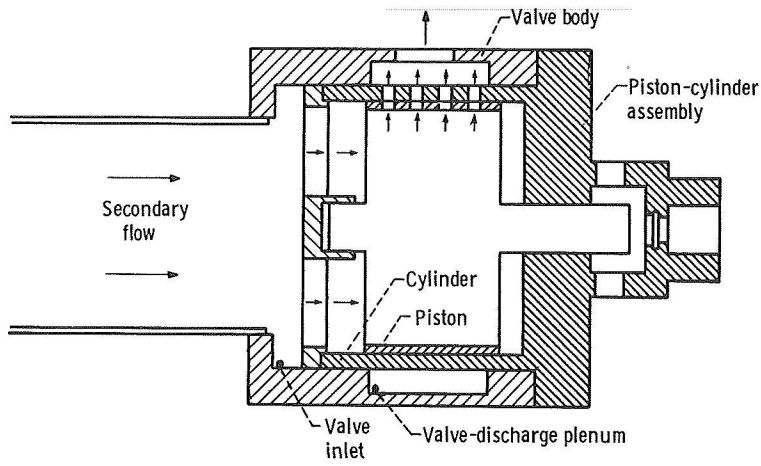
(b) Schematic drawing of primary test installation.

Figure 2. - Installation in test chamber.



C-68-2312

(a) Piston-cylinder assembly.



(b) Schematic cross section of flow-control valve.

Figure 3. - Servo-operated flow-control valve.

Secondary flow and flow-distribution control. - The butterfly-type valve in the secondary-air main supply line was available to control the nominal pressure at the inlet to the flow-control valves. Thus, both valve inlet pressure and valve-travel amplitude were available for amplitude control of the induced disturbances. For much of the steady-state evaluation reported herein, the piston-cylinder assemblies of the flow-control valves were not available and the butterfly valve provided control of secondary flow.

Circumferential distribution of the secondary air for inducing circumferential pressure distortions could be controlled in increments of 60° sectors by suitably controlling appropriate flow-control valves. Without the piston-cylinder assemblies of the flow-control valves, most of the steady-state circumferential distortions evaluated in the present investigation were achieved by blocking the secondary air in the line downstream of the torus manifold of selected 60° sectors.

Radial distribution of the secondary air was modified for inducing radial pressure distortions by removing those sections of the secondary-flow lines external of the inlet duct between the valve-discharge plenums and selected secondary nozzles. The resultant openings were capped.

Primary-Air System and Installation

The experimental evaluation was conducted in an altitude test chamber of the Lewis Propulsion System Laboratory. The primary test installation (fig. 2) was of a conventional direct-connect type. The altitude facility includes a forward bulkhead which separates the inlet plenum from the test chamber. Conditioned primary air was supplied to the inlet plenum at the desired pressure and temperature. The test chamber aft of the bulkhead was evacuated to the desired exhaust pressure. The exhaust pressure was maintained constant by an automatic valve.

The conditioned primary air flowed from the facility inlet plenum through a bellmouth and the inlet duct to the normal engine compressor-inlet location. The bellmouth and inlet duct were from a TF-30 engine program (ref. 3). Most of the evaluation reported herein was accomplished while using a duct extension to replace the engine. For this case, changeable choked flat-plate orifices were installed in the duct extension and provided control of total airflow. Exhaust from the duct or engine was captured by a collector which extended through a rear bulkhead.

Instrumentation

Steady-state measurements. - Instrumentation from the TF-30 engine program of

reference 3 was used in the inlet duct to determine inlet primary airflow rates and pressures upstream and downstream of the secondary-air injection hardware (figs. 1 and 2). Primary-air temperature was measured at the bellmouth entrance. Total pressures, including the boundary layer, and wall-static pressures were measured at station 1. Total pressures (eight rakes) and wall-static pressures (inner and outer walls) were measured at station 2. Station 1 was nominally 95 inches (241 cm) upstream of station 2. In addition, with the duct extension replacing an engine, total pressures and temperatures were measured (at station D) forward of the flat-plate orifices used at the duct-extension exit.

In the secondary-air system, temperatures were measured in the main supply line upstream of the torus manifold. Pressures were measured in the torus manifold, at the flow-control valve inlet, and in the flow-control valve-discharge plenum (fig. 3(b)).

Transient measurements. - During most of the evaluation reported herein, 1/4-inch- (0.635-cm-) diameter transducers were located in 10 selected probes at station 2 (fig. 1(b)) to obtain high-response transient measurements of total pressures downstream of the secondary-air injection hardware. For a series of tests with the secondary-air jet system and an engine, similar transducers were located in the 40 available probes at station 2 to obtain a more detailed survey of total-pressure distribution during induced pressure oscillations. Similar transducers were used in the investigation reported in reference 3, which includes a description of the high-frequency pressure measurement system used in that and the present investigations.

In the secondary-air system, transducers were used to obtain high-response transient wall-static pressure measurements at the inlet and discharge of the flow-control valves (fig. 3(b)) and, for a few tests, in one flow line just upstream of a secondary-flow nozzle (in the outer circumferential ring, fig. 1(b)). Position transducers were used to obtain measurements of the location of the control-valve pistons.

PROCEDURE

Test Conditions

This investigation was conducted primarily at a nominal total pressure of 0.5 atmosphere at station 2; selected evaluations were also made at nominally 0.3 and 0.7 atmospheres. Primary air was supplied to the facility inlet plenum at pressures required to obtain the desired pressure at station 2. Secondary air was supplied to the test facility at nominal pressures up to 10 atmospheres and throttled as required to vary secondary flow. Secondary-air temperature was not controlled and ranged from about 60° to 100° F (16° to 38° C). Primary-air temperature was varied to approximately match the secondary-air temperature.

Steady-State Program

Calibration of flat-plate orifices at duct-extension exit. - Choked flat-plate orifices were used to control corrected total airflow for the testing with the duct extension. Data were obtained, without secondary airflow, over a range of orifice pressure ratios to determine the requirements for choked-orifice flow and the corrected total airflow set by each orifice (based on airflow measured at station 1).

Secondary airflow calibration. - Secondary airflows were determined from measurement of the secondary-air inlet temperature and the pressures at the control-valve discharge plenums and use of a flow constant (based on a calibration and the assumption of choked secondary nozzles). The secondary nozzles were choked except at low flows, which were generally avoided. The calibration was accomplished by obtaining data over a range of secondary flows (with flow from all 54 secondary nozzles), and taking the difference between total flow and primary flow as a measure of secondary flow. The resultant data were used to determine an average flow constant for the case of assumed uniform flow from 54 secondary nozzles. For the distortion testing, the percentage of secondary nozzles in use was considered in determining secondary flow.

Uniformly distributed secondary flow. - Data were obtained over a range of uniformly distributed secondary flow at one corrected total flow to evaluate total-pressure profiles at station 2 with (1) upstream injection of the secondary air at injection planes 20.4 and 31 inches (51.8 and 78.8 cm) forward of station 2 and (2) downstream injection of the secondary air at an injection plane 37 inches (94 cm) forward of station 2. With upstream injection 31 inches (78.8 cm) forward of station 2, similar data were obtained at two additional corrected total flows to further evaluate total-pressure profiles and the momentum-interchange pressure loss.

Nonuniformly distributed secondary flow. - The capability of the secondary-air jet system for inducing circumferential pressure distortions was evaluated over a range of secondary flows with flow only from (1) three adjacent 60° sectors of secondary nozzles to provide a nominal 180° pressure distortion and (2) one 60° sector to provide a nominal 60° distortion. Data were obtained at each of three corrected total airflows.

The capability of the secondary-air jet system for inducing radial pressure distortions was evaluated over a range of secondary flows with flow only from (1) the outer circumferential ring of 24 secondary nozzles to provide a tip-radial distortion and (2) the inner circumferential ring of 12 secondary nozzles to provide a hub-radial distortion. Tip-radial distortions were evaluated at three corrected total airflows, whereas hub radial distortions were evaluated at but one corrected total airflow.

Transient Program

The capability of the secondary-air jet system for inducing dynamic uniform pressure oscillations was evaluated with equal synchronized oscillatory operation of the six high-response servo-operated flow-control valves at various discrete frequencies from 1 to as high as 200 hertz. The tests were made primarily at one corrected total airflow and average total pressure, with checks made at higher and lower pressures and one reduced corrected total flow. For most of this testing, the duct extension was used. The flat-plate orifices for corrected total flow control were repositioned forward to a location nominally 25.75 inches (65.4 cm) aft of station 2 to provide inlet-duct dynamic characteristics more representative of those with an engine installation (ref. 4). Some testing was accomplished with 40 transducers at station 2 during engine testing to evaluate in greater detail the uniformity of pressure during the pressure oscillations.

Flow Definitions

For the results presented herein, corrected total airflow was assumed to remain constant with a given duct orifice regardless of the secondary airflow or distribution. Corrected total airflow is expressed as a fraction of a "rated" value. The rated value was arbitrarily defined as that corrected airflow which would result in a one-dimensional Mach number of 0.500 in the annular area of the inlet duct. Steady-state corrected secondary airflow was corrected on the basis of the secondary-air temperature and the pressure in the inlet duct at station 2 and is expressed as a fraction of rated corrected total airflow. (Symbols are defined in appendix A.)

RESULTS AND DISCUSSION

Steady-State Uniformly Distributed Secondary Flow

Injection plane and flow direction. - With uniform secondary airflow from all the nozzles, it was considered necessary to achieve uniform total-pressure distribution at station 2. Appreciable total-pressure distortion for this case would diminish the potential usefulness of the system for inducing steady-state or dynamic compressor-inlet pressure disturbances. This would be true because of the difficulties in defining the particular compressor-inlet conditions as well as in analyzing and understanding the resultant effect on compressor-system characteristics or operating limits.

Data are presented in figure 4 to illustrate the influence of secondary-air injection-plane location and flow direction on total-pressure uniformity at station 2. The ratio of

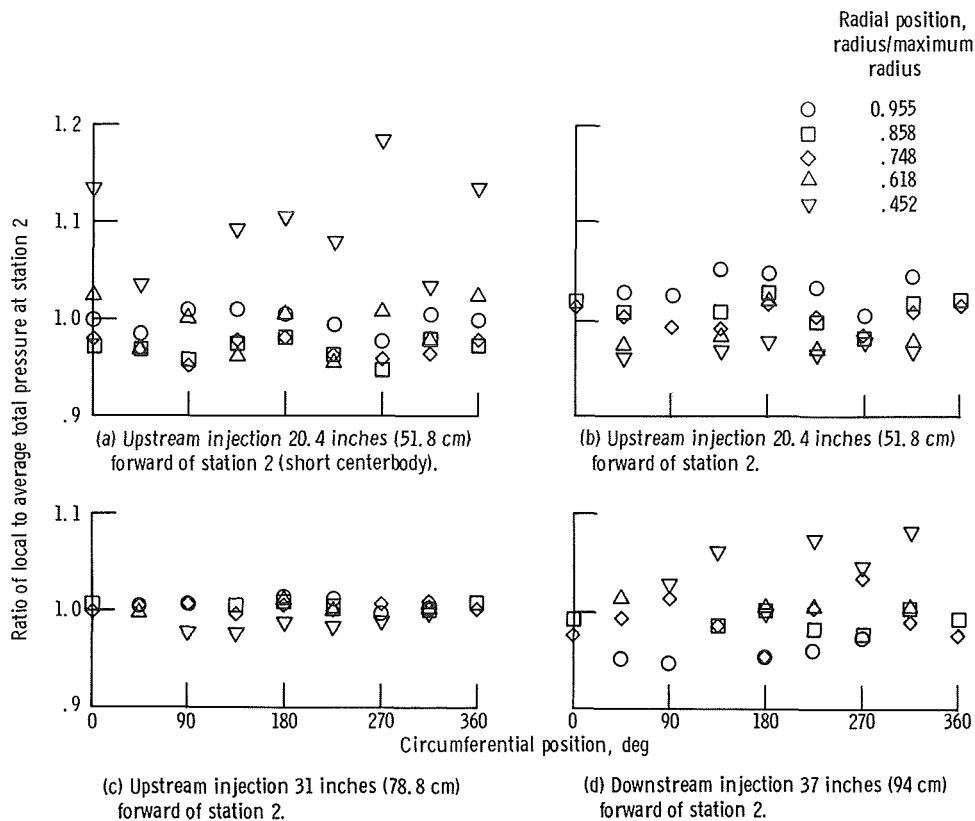


Figure 4. - Total-pressure distributions at station 2 with flow from all secondary nozzles; corrected total and secondary flows, 1.053 and 0.38 to 0.41 of rated corrected total flow.

local to average pressure is shown as a function of circumferential position for various radial probe positions. Corrected total and secondary flows were about 1.05 and 0.38 to 0.41, respectively, of rated corrected total flow.

The first test with upstream injection was made while using a short centerbody which extended only to, rather than through, the secondary injection plane. The resultant high pressure in the hub region is evident in figure 4(a), and illustrated the importance of uniformly mixing secondary and primary air. This was as would be expected.

With upstream injection and the longer centerbody configuration, there was a significant improvement in total-pressure uniformity when the mixing length was increased by moving the injection plane from 20.4 inches (51.8 cm) (fig. 4(b)) to 31 inches (78.8 cm) (fig. 4(c)) forward of the instrumentation survey plane. With the forward injection plane, there was a small radial profile but basically a flat circumferential profile; the total-pressure uniformity was considered to be acceptable.

With downstream injection for the one mixing length evaluated (37 in. or 94 cm), the total-pressure uniformity was not acceptable (fig. 4(d)). The three highest pressures measured were directly in line with secondary nozzles, which suggest that there were

54 high-pressure regions (54 nozzles). It was expected that adequate mixing of the secondary and primary air would be more difficult to achieve with downstream, as compared to upstream, injection.

On the basis of these results, upstream injection at the forward plane (with a center-body which extended through the injection plane) was selected for further evaluation studies to be discussed hereinafter.

Secondary and total flow effects. - Data are presented in figure 5 to illustrate the influence on total-pressure uniformity of (1) varying secondary flow at one total flow (figs. 5(a) to (c)) and (2) varying total flow at relatively high secondary flow (figs. 5(c) to (e)).

At 1.05 of rated corrected total flow without secondary flow (fig. 5(a)), there was a

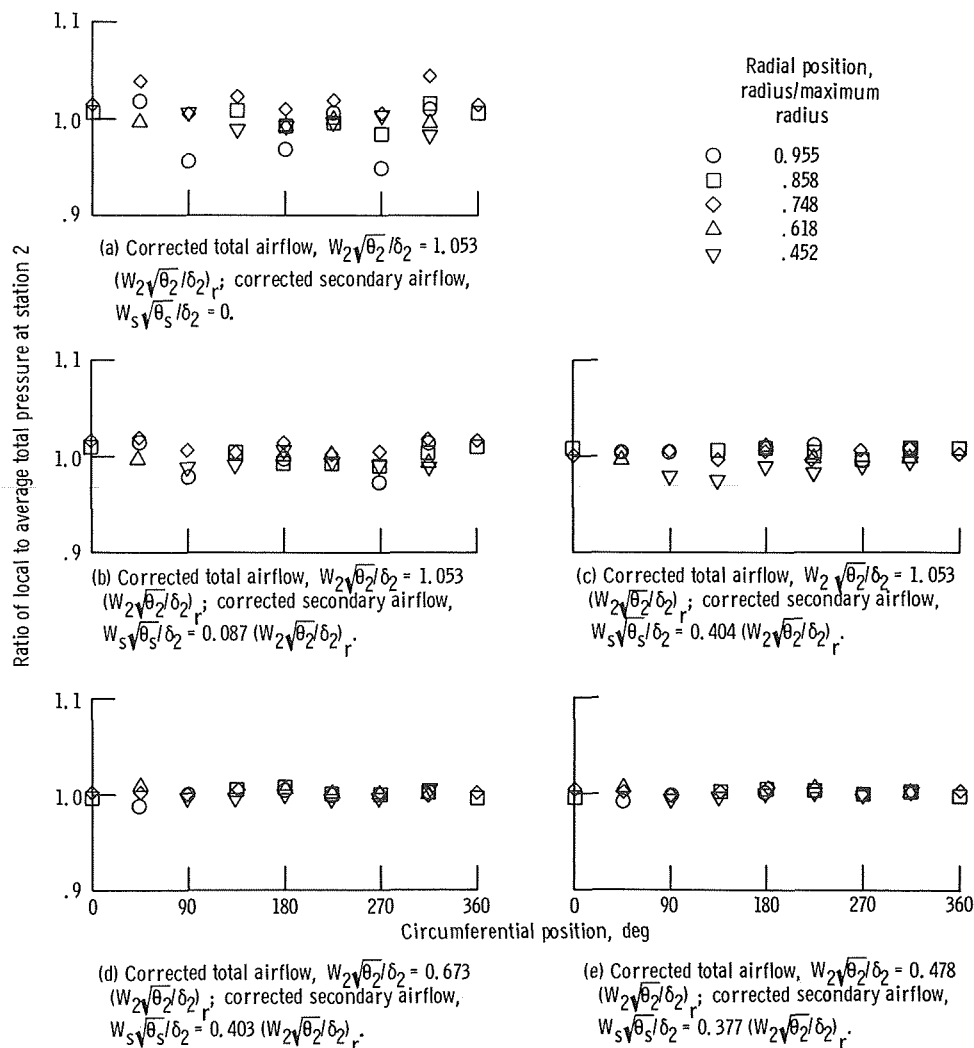


Figure 5. - Total-pressure distributions at station 2 with flow from all secondary nozzles; upstream injection 31 inches (78.8 cm) forward of station 2.

total-pressure spread of about ± 0.05 due primarily to wakes from the jet array hardware; this pressure spread diminished at lower total flows (not shown). With corrected secondary flows of about 0.09 (which was near minimum for choking with the particular secondary nozzles) and 0.40 of rated corrected total flow (figs. 5(b) and (c)), the total-pressure uniformity was considered to be acceptable and was somewhat improved over the case of no secondary flow. It will also be noted that total-pressure uniformity was even better at the reduced corrected total flows (figs. 5(d) and (e)).

Data are presented in figure 6 to illustrate the total-pressure distribution at station 2 for the case of a clean inlet (without the jet-array hardware) at three levels of

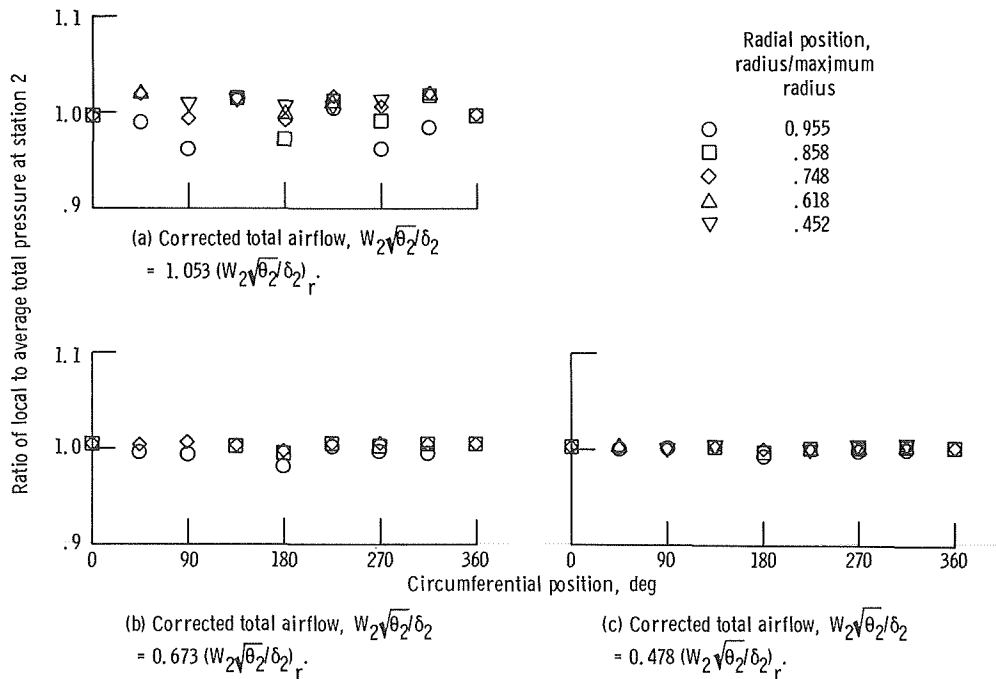


Figure 6. - Total-pressure distributions at station 2 with clean inlet (without jet-array hardware).

corrected airflow. With secondary airflow from the jet-array hardware, the total-pressure distribution (fig. 5) was essentially equivalent to that of the clean inlet (fig. 6).

Total-pressure loss due to jet-array hardware. - The total-pressure loss due to the jet-array hardware as a function of corrected airflow is shown in figure 7 and compared with the pressure loss of the clean inlet duct. With the jet-array hardware, the pressure losses ranged from 0.007 to 0.039 for corrected inlet airflows from 0.48 to 1.05 of rated; the clean-inlet-duct losses were from 0.001 to 0.005. These pressure losses due to the jet-array hardware were not a problem to the application.

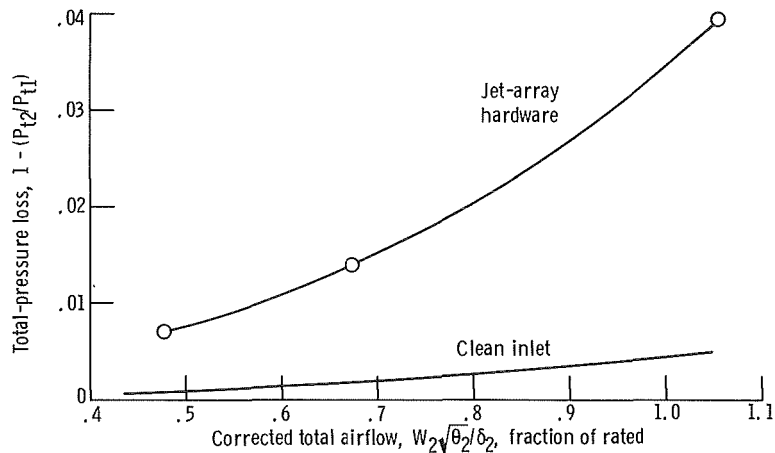


Figure 7. - Total-pressure loss in inlet duct with and without jet-array hardware; secondary airflow, $W_s = 0$.

Total-pressure loss with upstream injection of secondary air. - The total-pressure losses $1 - (P_{tB}/P_{tA})$ (not including losses due to the jet-array hardware) resulting from upstream injection of secondary air, counter to the primary air, are shown in figure 8 as a function of corrected secondary flow. Results from analysis and experiment are included for three corrected total airflows, with the analytical results represented by the curves and the experimental results by the data points. Analytically, P_{tB}/P_{tA} was determined through use of equations and assumptions presented in appendix B. Experimentally, P_{tB}/P_{tA} was determined from the ratio of P_{t2}/P_{t1} with secondary flow to the average P_{t2}/P_{t1} without secondary flow.

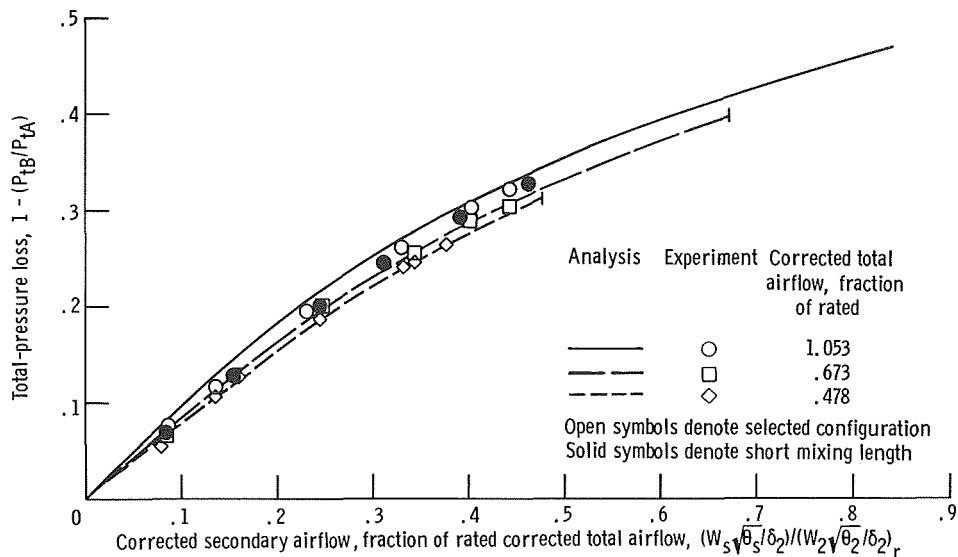


Figure 8. - Total-pressure loss with uniform upstream injection of secondary air, counter to primary air, in inlet duct; does not include loss due to hardware.

Momentum interchange between the secondary and primary air in the inlet duct upstream of the jet array resulted in total-pressure losses which increased, at a decreasing rate, as the corrected secondary flow was increased. Thus, induced total-pressure losses may be controlled by varying secondary airflow. At a given corrected secondary flow, the total-pressure losses increased somewhat as corrected total flow (Mach number) was increased. The experimental and analytical results are in good agreement, particularly at the two lower corrected total airflows. At a given corrected total airflow, the maximum usable total-pressure loss would occur when the secondary airflow is equal to the total airflow, for which case the upstream primary airflow and Mach number are zero and the upstream momentum is equal to $P_{tA} A_A$. The analytical curves for the two lower corrected total airflows have been extended to the condition of secondary flow equal to total flow.

Time-variant total pressure with steady-state secondary flow. - The injection of secondary air from a high-pressure source counter to primary air at relatively low pressure in the inlet duct could result in time-variant pressures, downstream of the momentum interchange between the two flows, even with steady-state flows. Appreciable amplitude of pressure variations would diminish the usefulness of the secondary-air jet system for inducing steady-state and, possibly, cyclic compressor-inlet pressure disturbances because of the difficulties of defining the particular conditions and of analyzing and understanding the resultant effect on the compressor system.

Average true root-mean-square (TRMS) pressure amplitude as a function of corrected secondary flow is presented in figure 9 for three corrected total flows. These data were obtained while using the duct extension with flat-plate orifices at the duct exit; inlet-duct dynamic characteristics, therefore, were probably not representative of those with an engine installation. The measured TRMS pressure variations show a trend of in-

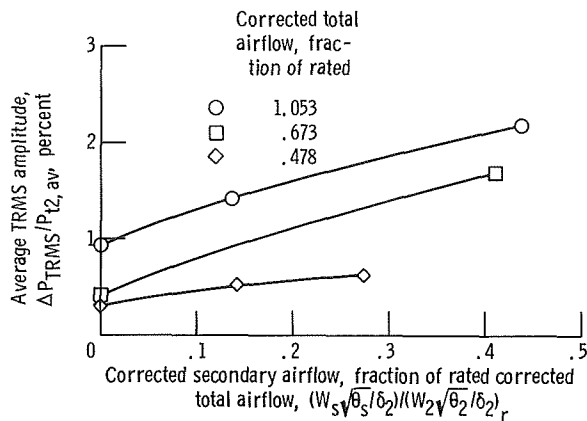


Figure 9. - Average true-root-mean-square (TRMS) pressure variation with steady-state upstream injection of secondary air 31 inches (78.8 cm) forward of station 2; frequency band, 0 to 500 hertz.

creased amplitude as secondary flow was increased at given total flows and as total flow was increased at given secondary flows. The levels, however, are not considered excessive. Comparable data are not available with a clean inlet. It can be stated, however, that use of the secondary-air jet system in engine programs has shown no detrimental influence of TRMS pressure variations on compressor-system operating limits.

Steady-State Nonuniformly Distributed Secondary Flow

Circumferential pressure distortions. - Total and wall-static pressure distributions at station 2, with secondary airflow from only three adjacent 60° sectors of secondary nozzles, are illustrated for selected corrected secondary airflows at each of three corrected total airflows in figures 10(a) to (c). The ratio of local pressure to average total pressure is presented as a function of circumferential position for various radial probe positions.

The total pressure and Mach number, aft of the nozzles with secondary flow, were progressively depressed relative to the average as the secondary flow was increased. The circumferential extent of the below-average total pressure was generally greater than 180° . The available range of secondary airflow was such that it was possible to stagnate the flow aft of the secondary flow at the lower corrected total flows. The measured pressures indicate that further increase in secondary flow beyond the initial stagnation condition resulted in further depression of the pressures behind the secondary flow and increased pressures and Mach number behind the nozzles without secondary flow. Total pressures were quite uniform aft of the nozzles with secondary flow, but somewhat nonuniform aft of nozzles without secondary flow due to wakes from the jet array hardware. Though it is not illustrated, it is believed that the uniformity of pressures in the high-pressure region would be improved through use of low secondary airflow through the nozzles in that region. Effectively, the circumferential distortions could be obtained by differential throttling of the 60° sectors.

For secondary airflow from only one 60° sector of secondary nozzles, total and wall-static pressure distributions at station 2 are illustrated for selected corrected secondary airflows at the three corrected total airflows in figures 11(a) to (c). Again the total pressures and Mach number aft of the nozzles with secondary flow were depressed relative to the average. As the secondary airflow was increased, the circumferential extent of the below-average total-pressure region increased. At the highest total corrected airflow, minimum total pressures decreased progressively as secondary airflow was increased at least to the point of locally stagnated flow. At the two low total corrected airflows, total pressures in the low-pressure region reached a minimum level relative to average pressure at low secondary airflows; further increased secondary flow increased the circumferential extent but not the level of the depressed pressures in

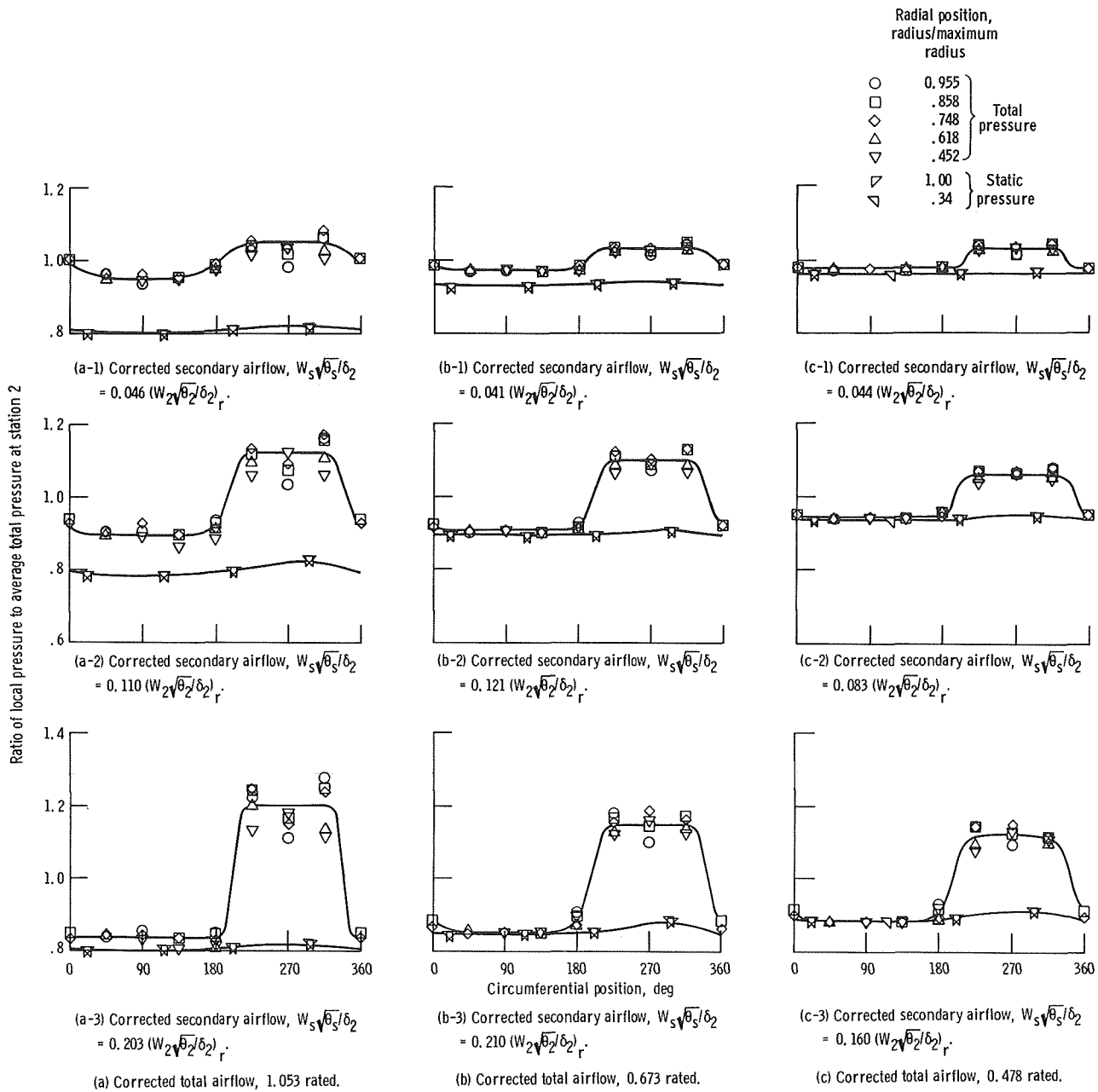


Figure 10. - Circumferential pressure distortion; secondary flow from three adjacent 60° sectors.

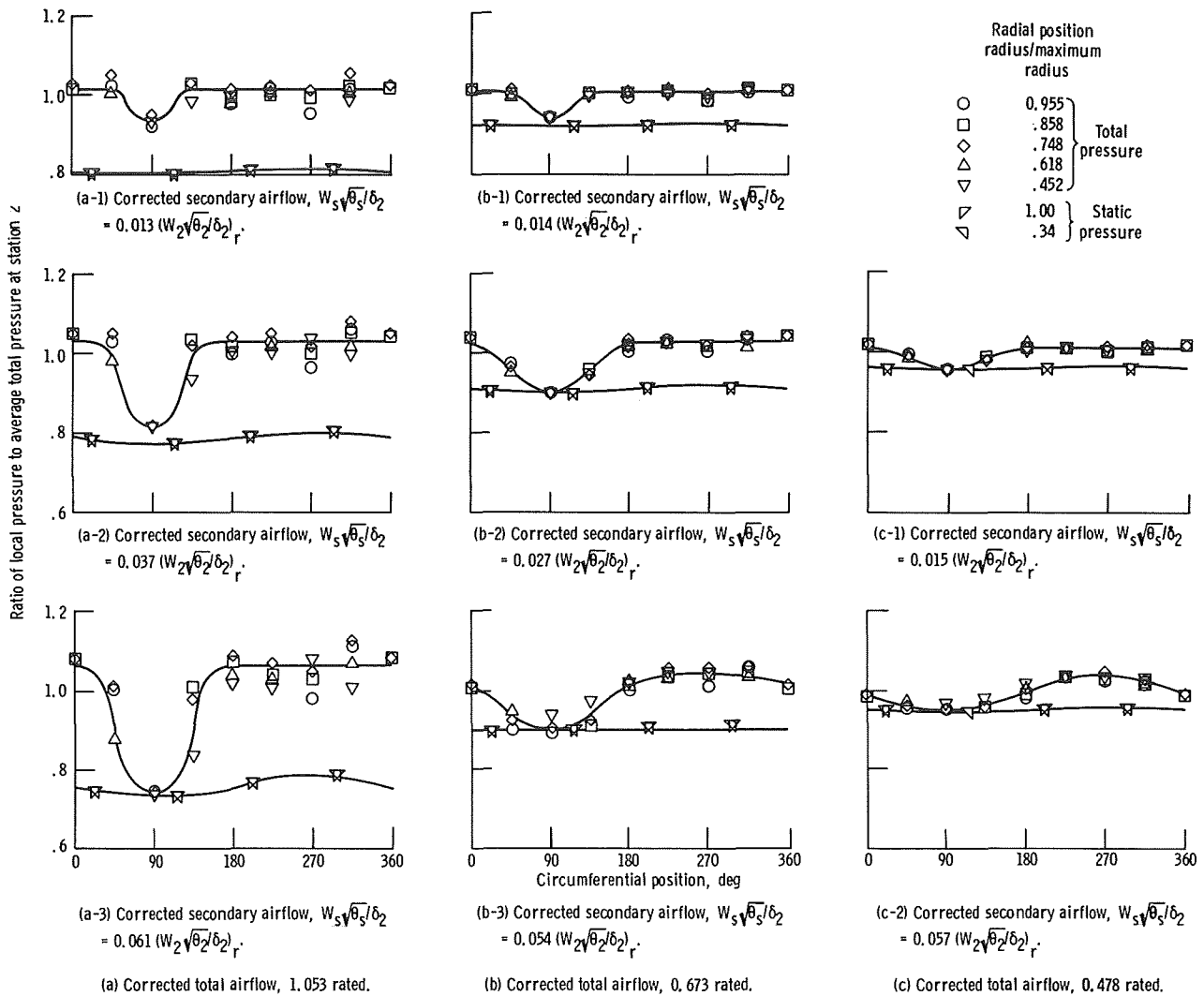


Figure 11. - Circumferential pressure distortion; secondary flow from one 60° sector.

this stagnated flow region. The circumferential extent of the below-average pressure region reached close to 180°.

Radial pressure distortions. - Total- and wall-static pressure distributions at station 2, with secondary flow from only the outer circumferential ring of 24 secondary nozzles, are illustrated for selected corrected secondary airflows at each of three corrected total airflows in figures 12(a) to (c). With secondary airflow, total pressures in the tip region were depressed and those toward the hub were increased relative to the average total pressure. As the secondary airflow was increased, the pressures in the tip region were further depressed, and the radial extent of the below-average pressure region was increased somewhat. The range of available secondary airflows was such that it was possible to stagnate the flow aft of the secondary flow in the tip region at relatively high secondary airflow.

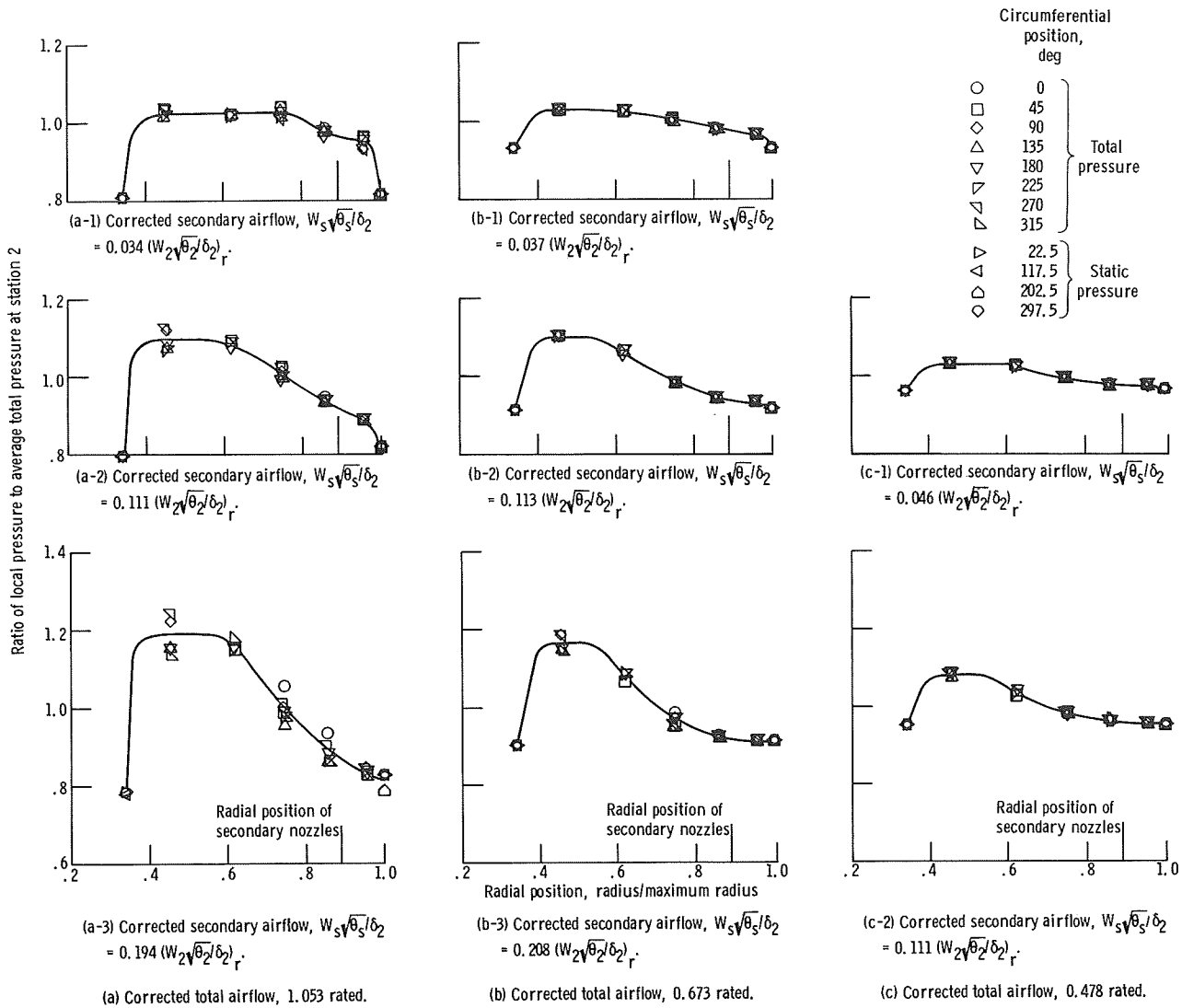


Figure 12. - Tip-radial pressure distortion; secondary flow from outer circumferential ring.

With secondary airflow from only the inner circumferential ring of 12 secondary nozzles, total- and wall-static pressure distributions at station 2 are illustrated in figure 13 for selected corrected secondary airflows at one corrected total airflow. With secondary airflow, total pressures in the hub region were depressed and those towards the tip were increased relative to the average total pressure. As secondary airflow was increased, the pressures in the hub region were further depressed. The range of available secondary flows was such that it would be possible to stagnate the flow aft of the secondary flow in the hub region, particularly at lower corrected total flows (for which data were not obtained).

Distortion amplitude control. - The data of figures 10 to 13 indicate that the secondary-air jet system can be used to induce variable-amplitude steady-state circum-

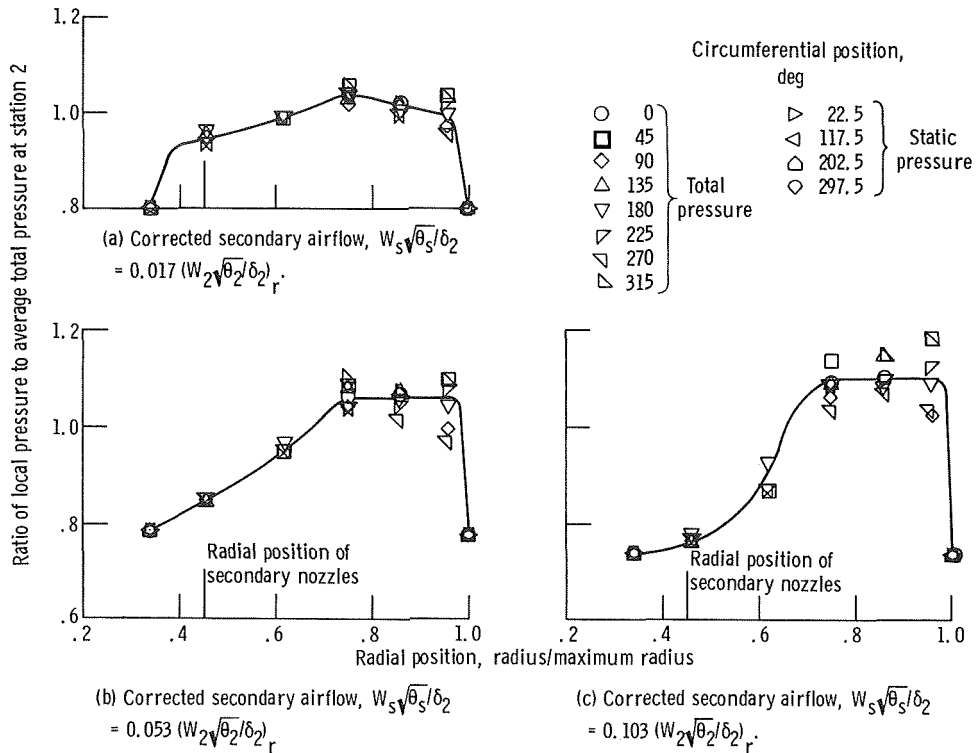


Figure 13. - Hub-radial pressure distortion; secondary flow from inner circumferential ring; corrected total airflow, 1.053 rated.

ferential and radial pressure distortions. To further illustrate the control of distortion amplitude through control of secondary flow, distortion amplitude $1 - (P_{t2, \min} / P_{t2, \text{avg}})$ is presented as a function of a corrected secondary flow parameter

$\left[\left(W_s \sqrt{\theta_s / \delta_2} \right) \left(N_{s, \text{max}} / N_s \right) \right]$ in figure 14. Data are included for the circumferential and radial distributions of secondary flow previously illustrated at the three corrected total flows.

Distortion amplitude progressively increased as secondary flow was increased (in most cases) and as corrected total flow was increased at a given value of the corrected secondary flow parameter. In the case of secondary flow from only one 60° sector of nine secondary nozzles, maximum distortion amplitude was obtained at low secondary flow. As was previously indicated in this case, the flow aft of the secondary flow stagnated at low secondary flow, and further increased secondary flow extended the circumferential extent without influencing distortion amplitude.

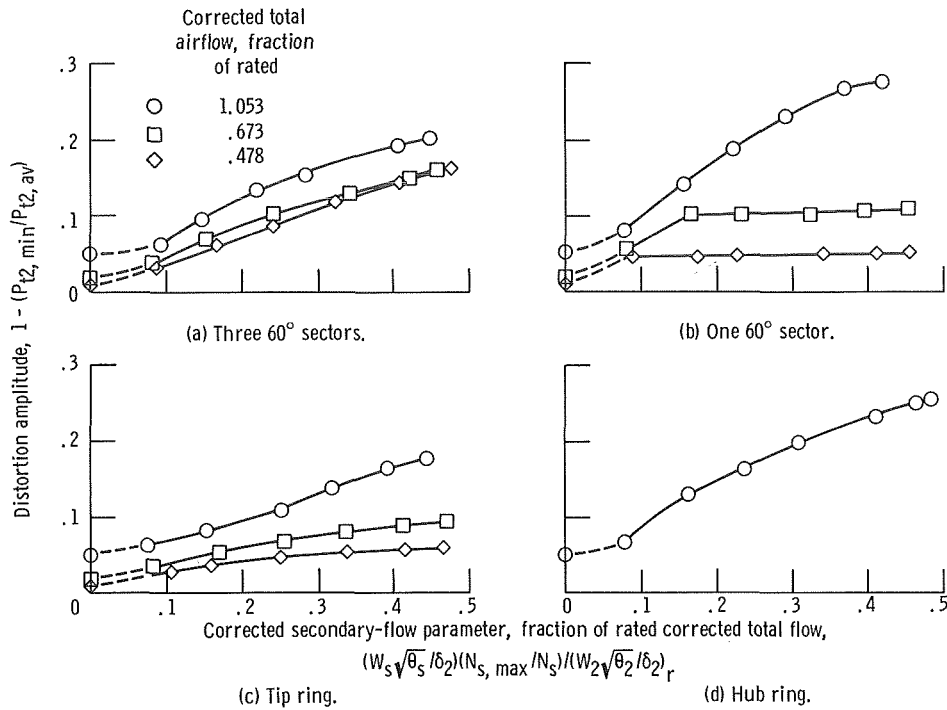


Figure 14. - Distortion amplitude control through control of secondary flow.

Dynamic Uniformly Distributed Pressure Oscillations

Characteristics of flow-control valves. - The flow-control valves provided control of induced pressure disturbances at station 2 through control of secondary flow. With a given pressure at the valve inlet, secondary flow control was achieved by control of valve-port area. For the particular combination of flow-control valves and secondary flow lines and nozzles used in this evaluation, the flow-control characteristics of the valves were nonlinear. The approximate variation of steady-state secondary flow and total-pressure loss in the primary duct as a function of valve-port area are illustrated in figure 15 for the case of six valves in use. The pressure loss curve was constructed from the secondary flow curve and the data from figure 8 for 1.05 of rated corrected total flow. Secondary flow and induced pressure losses both varied nonlinearly with valve-port area. It is apparent from these steady-state characteristics that, with oscillatory operation of the valves, the wave shape of induced pressure oscillations in the inlet duct will be influenced by the region of valve-port area in which the control valves are oscillated. There is potential for varying the induced-pressure oscillatory waveform, if desired.

In the initial evaluation of oscillatory valve operation, the valves were oscillated an equal extent about various midpositions. As would be expected from the approximate

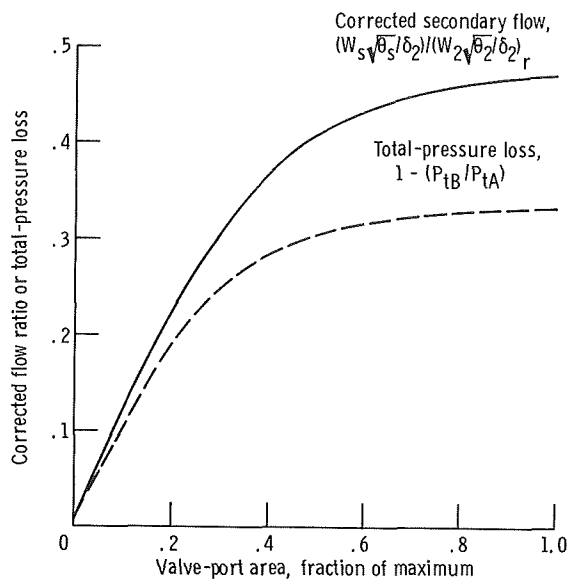


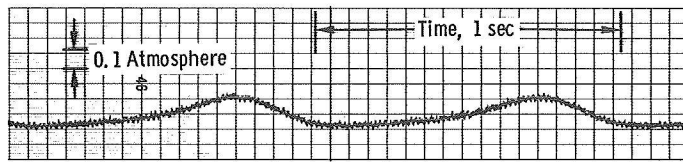
Figure 15. - Typical characteristics with flow-control valves.

steady-state characteristics, oscillatory operation of the valves about midpositions corresponding to 0.26 to 0.34 of maximum valve-port area was found to provide the best compromise as to symmetry of oscillatory induced-pressure waveform and disturbance amplitude. To avoid any mechanical interference problems (a potential when oscillating the valves to the full-closed position at high frequencies) oscillatory valve operation between the limits of 0.1 and 0.58 (0.34 ± 0.24) of maximum valve-port area was selected.

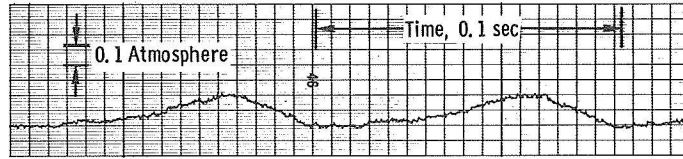
Uniform induced-pressure oscillations. - Uniform induced-pressure oscillations at station 2 in the inlet duct were evaluated through synchronized equal oscillatory operation of the control valves to dynamically vary secondary flow at constant corrected total flow. The total pressure upstream of the momentum interchange in the inlet duct was set at a preselected level and not controlled (nor measured dynamically). Data were obtained at various discrete frequencies of control valve oscillation.

Sample records of total pressure at station 2 as a function of time for selected oscillatory frequencies of the control valves are shown in figure 16. In addition, approximate typical variations of station 2 total pressure as a function of fraction of a cycle for one cycle are shown in figure 17 for selected oscillatory frequencies; these data were obtained at a corrected total airflow of 1.05 of rated flow. The induced-pressure-variation waveform was not symmetrical, as expected, but was considered to be reasonable. Amplitude of the induced-pressure variation was good at very low frequencies, but severely attenuated at higher frequencies.

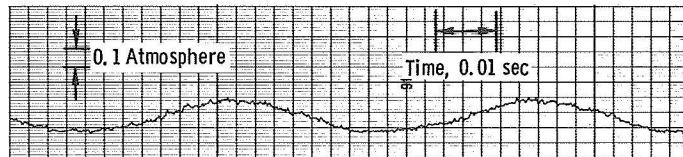
Amplitude characteristics of the induced-pressure oscillations are further illustrated in figure 18 in terms of amplitude ratio as a function of oscillatory frequency.



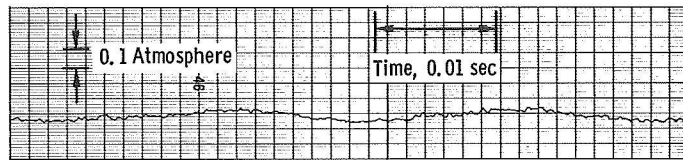
(a) Frequency, 1 hertz.



(b) Frequency, 10 hertz.



(c) Frequency, 20 hertz.



(d) Frequency, 40 hertz.

Figure 16. - Sample records of induced oscillatory total pressure, P_{t2} .

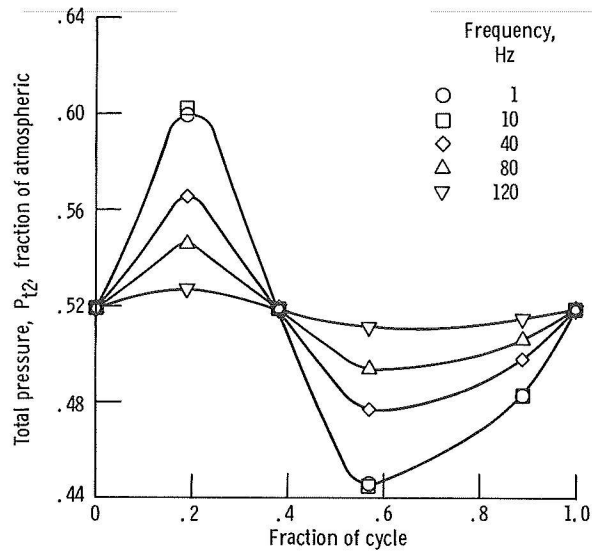


Figure 17. - Induced oscillatory total pressure, P_{t2} ; corrected total airflow, 1.053 rated.

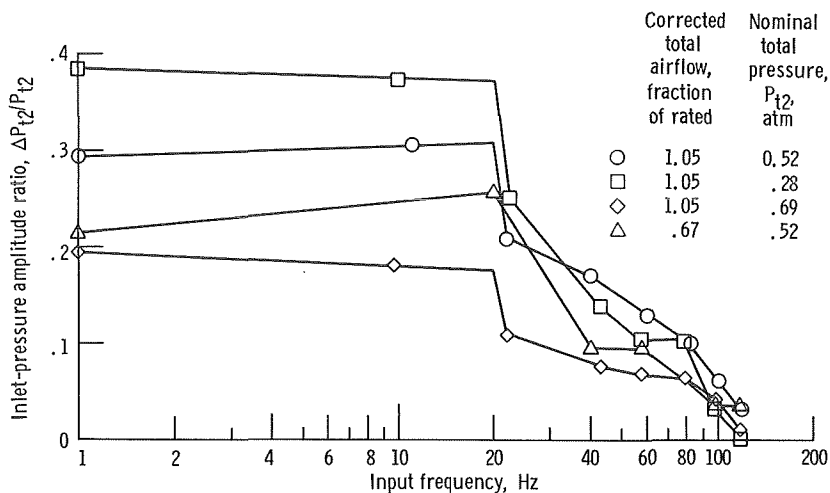


Figure 18. - Inlet-pressure amplitude characteristics.

Data are included from operation at nominal pressures of 0.28, 0.52, and 0.69 atmosphere with 1.05 rated corrected total flow, and a nominal pressure level of 0.52 atmosphere with 0.67 of rated corrected total flow. In all cases, near maximum amplitude for the particular conditions was available to a frequency of only 20 hertz, and experience indicated a sharp reduction in maximum amplitude just above 20 hertz. There was essentially continuous amplitude attenuation over the frequency range from just above 20 to 120 hertz. On a relative basis, the greatest attenuation was at the lowest pressure level. Maximum amplitude in the low-frequency range decreased as the nominal pressure level was increased because of the reduced proportion of total flow available from the secondary flow system. Maximum amplitude in the low-frequency range decreased as corrected total flow was reduced, probably because of the reduced Mach number in the inlet duct; it was previously noted that reduced steady-state pressure losses occurred at reduced corrected total flows for a given corrected secondary flow.

The amplitudes available in the low-frequency range were considered to be of sufficient interest that the identical secondary-air jet system was used in an engine program. It is considered of interest that the amplitude and amplitude attenuation characteristics illustrated herein (from tests with a duct rather than an engine) are representative of those observed during the engine program. Thus, inlet-duct dynamics were similar for the duct (with the choked orifice located a short distance aft of station 2) and engine tests.

The uniformity of pressures at station 2 during induced-pressure oscillations was evaluated through use of up to 40 pressure transducers during the engine program. The variation of these pressures during one oscillatory cycle is illustrated in figure 19 for a frequency of 10 hertz. The distortion amplitude $1 - (P_{t2, \min}/P_{t2, \text{avg}})$ during the cycle ranged from 0.014 to 0.025 and averaged 0.019. It is apparent that the oscillatory pressures were basically uniform circumferentially and radially. Thus, uniform pressure

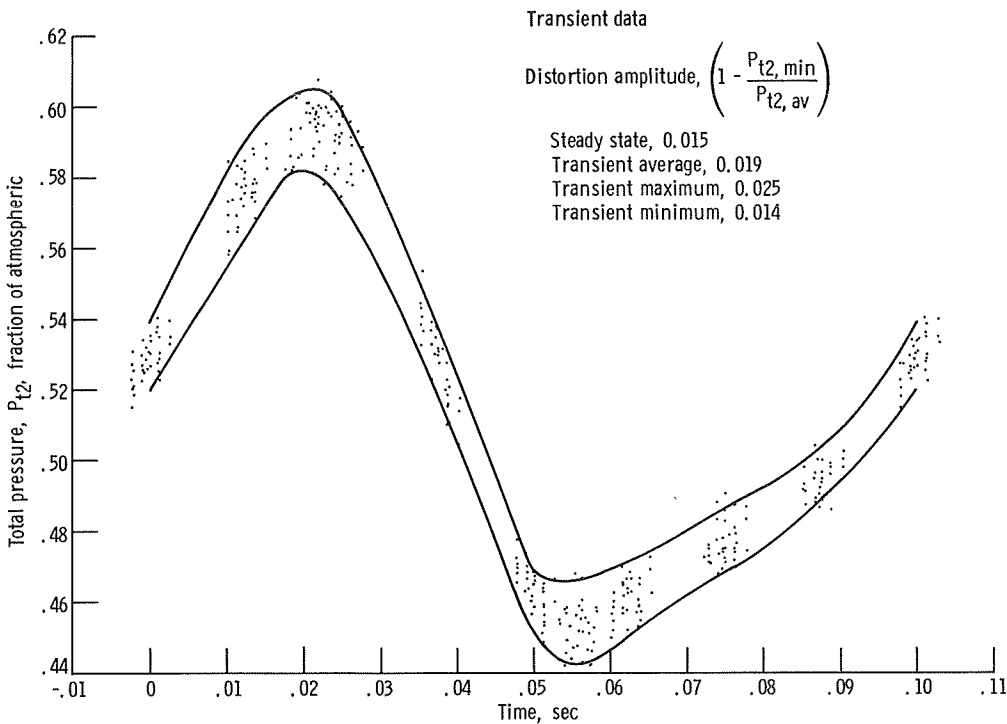


Figure 19. - Typical variation of engine inlet pressure during a uniform cyclic pressure oscillation; frequency, 10 hertz.

oscillations can be induced in the inlet duct through use of the secondary-air jet system, at least at low frequencies, without appreciable superimposed pressure distortions.

Power spectral density (PSD) during induced pressure oscillations is illustrated in figure 20 for a selected frequency. The level was low except at or near the oscillatory input frequency. The narrow sharp PSD spike at the input frequency suggests that pressure oscillations of discrete frequency can be induced through use of the secondary-air jet system, at least in the low-frequency range.

Secondary-system pressure oscillations. - The flow lines from the torus manifold to the flow-control valves should be as short as possible for dynamic testing, but could not be suitably shortened in this investigation. Pressure at the control-valve inlet varied during oscillatory operation of the valves. The variation resulted in maximum valve-inlet pressure at minimum valve-port area and, conversely, minimum valve-inlet pressure at maximum valve-port area. Such pressure variations restrict maximum amplitude capabilities of the system. Orifices, inserted in the flow lines near the torus manifold, were used in the present investigation to minimize the valve-inlet pressure variations.

Pressures measured at the control-valve inlet and discharge and in one jet tube just upstream of the secondary nozzle are shown in figure 21 during one cycle at selected frequencies. The amplitude of the valve-inlet pressure variation attenuated at frequencies

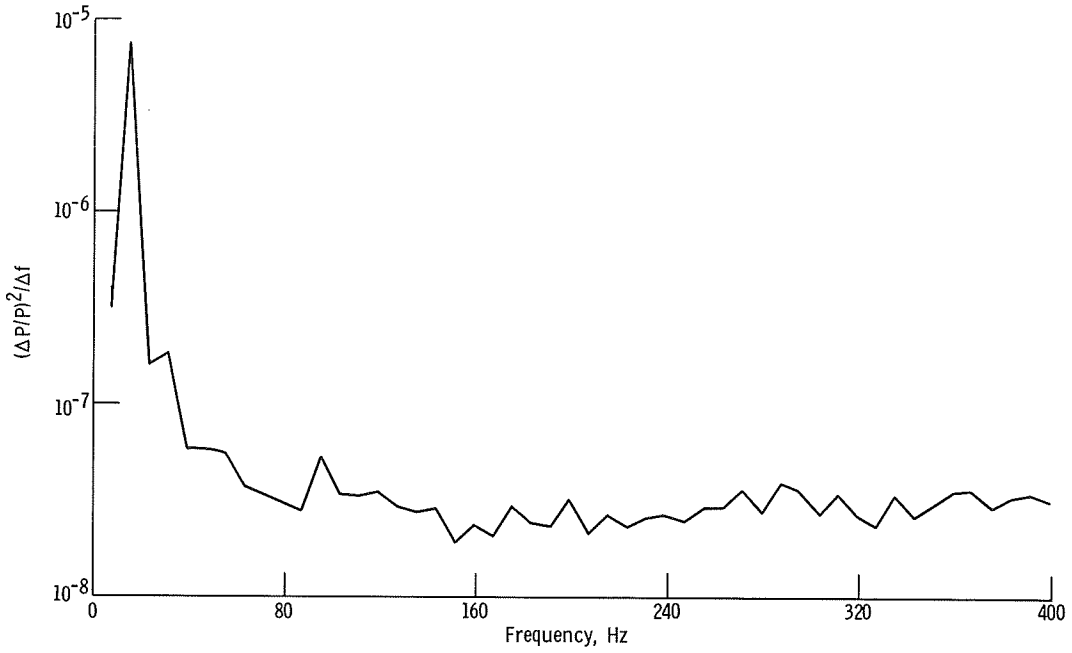


Figure 20. - Power spectral density (PSD) with induced-pressure oscillations at frequency of 15 hertz.

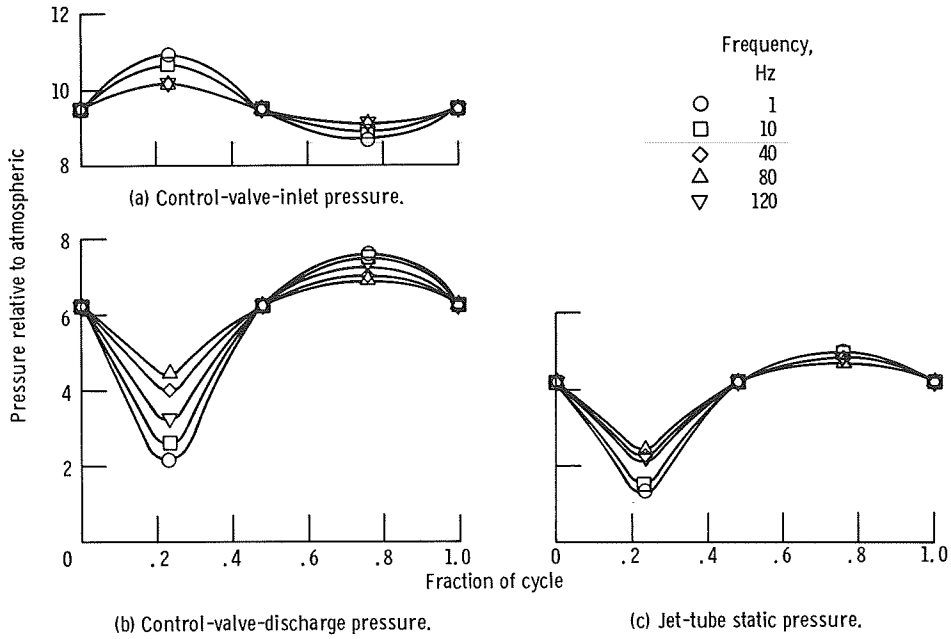


Figure 21. - Oscillatory pressures in secondary-air system.

from 1 to 40 hertz and appeared constant over the frequency range from 40 to 120 hertz. The amplitude of variation of the valve discharge and jet-tube pressures attenuated at frequencies from 1 to about 80 hertz, and the attenuation decreased as the frequency was increased to 120 hertz.

Amplitude attenuation. - Relative amplitude (amplitude ratio at any frequency relative to the amplitude ratio at a frequency of 1 Hz) of valve-discharge pressure, jet-tube static pressure, and pressures in the inlet duct aft of the jet array are compared over the frequency range investigated in figure 22. Amplification of pressures in the inlet duct at low frequencies (up to 20 Hz) are attributed to dynamics of the inlet duct. Attenuation of pressures in the inlet duct was the result of attenuations in both the secondary-air system and the inlet duct.

Modifications to the secondary-air jet system are planned in an attempt to minimize the amplitude attenuation in that system. The modifications planned include use of an enlarged torus manifold and near minimum length lines between the new manifold and the flow-control valves in an effort to minimize the valve-inlet pressure variations over the frequency range of interest. A jet array with enlarged flow lines and, therefore, greater secondary-flow capability is also being considered to provide greater dynamic amplitude capability.

It is considered likely that the amplitude of induced dynamic inlet pressure oscillations would be greater if the secondary flow were injected downstream rather than up-

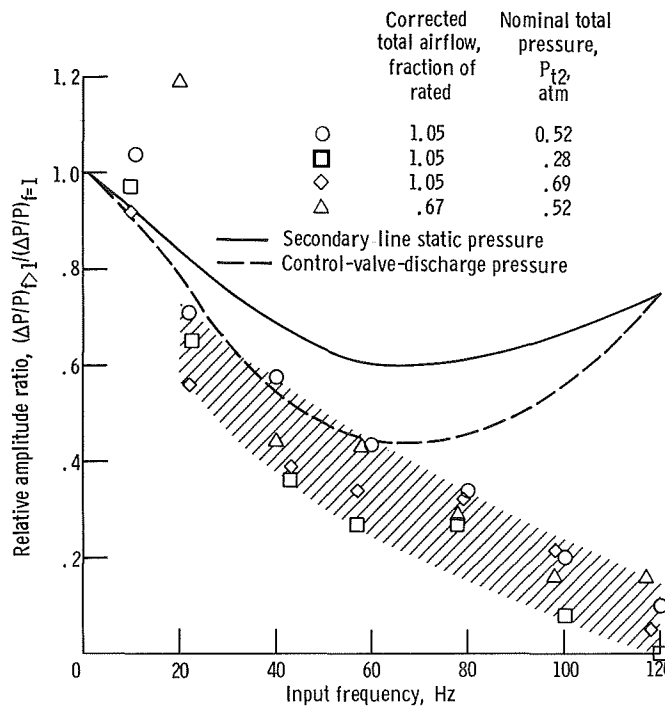


Figure 22. - Pressure amplitude attenuation characteristics.

stream. However, the uniformity of total-pressure distribution with downstream injection of the secondary flow must be improved appreciably over that of the steady-state flow case discussed earlier. Techniques of improving the pressure distribution with downstream injection are being studied experimentally.

Additional potential capabilities of servocontrolled valves. - Although only synchronized operation of the flow-control valves to induce uniform pressure oscillations in the inlet duct has been illustrated herein, the servocontrol system provides additional potential capabilities. These include use of the flow-control valves, for example, to induce (1) single pressure pulses of varied distribution (circumferential and radial), duration, and rate of change, (2) oscillatory pressure distortions of varied type through operation of only selected valves in synchronization or all valves with selected phase relations, (3) rotating pressure distortions through operation of a selected number of valves or all valves with selected phase relations, and (4) relatively random pressure disturbances (possibly) by using a tape-recorded random signal to control the valves. Capabilities of the system in all cases, of course, will be limited by the frequency response capabilities of the flow-control valves and the amplitude attenuation characteristics in the secondary-air jet system and the primary inlet duct.

CONCLUDING REMARKS

An investigation was conducted to evaluate a technique for inducing controlled steady-state and dynamic inlet pressure disturbances for jet engine tests. In this technique, secondary air was injected through an array of small nozzles uniformly distributed in the engine inlet duct to achieve momentum interchange with the primary air forward of the compressor face location. High-response servo-operated valves provided steady-state and dynamic control of secondary airflow.

The technique provides a convenient and acceptable way, through control of the secondary-air distribution and flow rate, of inducing variable-amplitude steady-state or dynamic pressure distortions (circumferential and radial) or dynamic uniform pressure oscillations without excessive random pressure amplitude. Dynamic pressure distortions were not evaluated in this investigation. The amplitude of induced dynamic pressure oscillations was reasonable at low frequencies but attenuated appreciably at frequencies above 20 hertz in this investigation. Work is currently in progress with the purpose of improving the amplitude capabilities of the particular technique at frequencies above 20 hertz.

Lewis Research Center,
National Aeronautics and Space Administration,
Cleveland, Ohio, October 17, 1969,
720-03.

APPENDIX A

SYMBOLS

A	area	Subscripts:	
m	mass flow	A, B	stations upstream and downstream, respectively, of momentum interchange between primary and secondary air
N_s	number of secondary nozzles		
P	static pressure		
P_t	total pressure	av	average
ΔP_{TRMS}	true-root-mean-square amplitude of random pressure variation	f	frequency
		max	maximum
T	total temperature	min	minimum
v	velocity	r	rated
W	weight flow	s	secondary
δ	ratio of average total pressure to standard sea-level static pressure	1, 2	stations 1 and 2
θ	ratio of average total temperature to standard sea-level static temperature		

APPENDIX B

ANALYSIS OF P_{tB}/P_{tA}

In the analysis, P_{tB}/P_{tA} (with uniform upstream injection of secondary air) was determined through use of the following equations which are based on momentum balance. It was assumed that the momentum interchange took place in a constant-area section of the inlet duct. Thus,

$$(P_{tA})_B \left(\frac{mv + PA}{P_{tA}} \right)_B + (P_{tA})_S \left(\frac{mv + PA}{P_{tA}} \right)_S - P_{tB} A_S = (P_{tA})_A \left(\frac{mv + PA}{P_{tA}} \right)_A \quad (1)$$

where $A_A = A_B = A_2$, and A_S is the summation of the throat areas of the secondary (convergent) nozzles. Without secondary flow, it was assumed that $(mv + PA)_B = (mv + PA)_A$ and $P_{tB} = P_{tA}$. With secondary flow, the net total momentum of the secondary flow was assumed to be $(mv)_S + A_S(P_S - P_{tB})$ or $(mv + PA)_S - P_{tB} A_S$. It was observed that whether $P_{tB} A_S$ or $P_{tB} A_S$ was used made little difference to the result; $P_{tB} A_S$ was used. From equation (1),

$$\begin{aligned} \left(\frac{mv + PA}{P_{tA}} \right)_B + \frac{(W\sqrt{T})_S}{(W\sqrt{T})_B} \left(\frac{W\sqrt{T}}{P_{tA}} \right)_B \frac{\left(\frac{mv + PA}{P_{tA}} \right)_S}{\left(\frac{W\sqrt{T}}{P_{tA}} \right)_S} - \frac{A_S}{A_B} &= \frac{(P_{tA})_A}{(P_{tA})_B} \left(\frac{mv + PA}{P_{tA}} \right)_A \\ &= \frac{(W\sqrt{T})_A}{(W\sqrt{T})_B} \left(\frac{W\sqrt{T}}{P_{tA}} \right)_B \frac{\left(\frac{mv + PA}{P_{tA}} \right)_A}{\left(\frac{W\sqrt{T}}{P_{tA}} \right)_A} \end{aligned} \quad (2)$$

$$\frac{\left(\frac{W\sqrt{T}}{P_t A}\right)_A}{\left(\frac{mv + PA}{P_t A}\right)_A} = \frac{\frac{\left(\frac{W\sqrt{T}}{P_t A}\right)_A \left(\frac{W\sqrt{T}}{P_t A}\right)_B}{\left(\frac{W\sqrt{T}}{P_t A}\right)_B}}{\left(\frac{mv + PA}{P_t A}\right)_B + \frac{\left(\frac{W\sqrt{T}}{P_t A}\right)_S \left(\frac{W\sqrt{T}}{P_t A}\right)_B}{\left(\frac{W\sqrt{T}}{P_t A}\right)_B} \frac{\left(\frac{mv + PA}{P_t A}\right)_S}{\left(\frac{W\sqrt{T}}{P_t A}\right)_S} - \frac{A_S}{A_B}} \quad (3)$$

$$\frac{P_{tB}}{P_{tA}} = \frac{\left(\frac{mv + PA}{P_t A}\right)_A}{\left(\frac{mv + PA}{P_t A}\right)_B + \frac{\left(\frac{W\sqrt{T}}{P_t A}\right)_S \left(\frac{W\sqrt{T}}{P_t A}\right)_B}{\left(\frac{W\sqrt{T}}{P_t A}\right)_B} \frac{\left(\frac{mv + PA}{P_t A}\right)_S}{\left(\frac{W\sqrt{T}}{P_t A}\right)_S} - \frac{A_S}{A_B}} \quad (4)$$

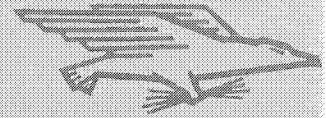
The terms $(mv + PA)/P_t A$ and $W\sqrt{T}/P_t A$ are Mach number functions. Equation (3) enabled determination of Mach number at station A and, therefore, $[(mv + PA)/P_t A]_A$ for use in equation (4). The values of $[(mv + PA)/P_t A]_S$ and $(W\sqrt{T}/P_t A)_S$ were based on sonic flow (choked secondary nozzles). The analysis was made for constant values of the Mach number functions at station B over a range of W_s/W_B ; the resulting curves were extended through the low-secondary-flow region (unchoked secondary nozzles) to the case of zero secondary flow. All temperatures were assumed to be equal. The following two relations enable solution of equations (3) and (4):

$$\text{or } \left. \begin{aligned} W_B - W_s &= W_A \\ W_2 - W_s &= W_1 \end{aligned} \right\} \quad (5)$$

$$\left(\frac{W\sqrt{T}}{P_t A}\right)_B = \left(\frac{W\sqrt{T}}{P_t A}\right)_2 \left(\frac{P_{t2}}{P_{tB}}\right) = \left(\frac{W\sqrt{T}}{P_t A}\right)_2 \left(\frac{P_{t2}}{P_{t1}}\right)_{W_s=0} \quad (6)$$

REFERENCES

1. Gabriel, D.; Wallner, L.; Lubick, R.; and Vasu, G.: Some Effects of Inlet Pressure and Temperature Transients on Turbojet Engines. *Aeron. Eng. Rev.*, vol. 16, no. 9, Sept. 1957, pp. 54-59, 68.
2. Kimzey, W. F.: An Investigation and Calibration of a Device for the Generation of Turbulent Flow at the Inlet of a Turbojet Engine. ARO, Inc. (AEDC-TR-65-195, DDC No. AD-472210), Oct. 1965.
3. Braithwaite, W. M.; and Vollmar, W. R.: Performance and Stall Limits of a YTF30-P-1 Turbofan Engine with Uniform Inlet Flow. NASA TM X-1803, 1969.
4. Wasserbauer, Joseph F.; and Willoh, Ross G.: Experimental and Analytical Investigation of the Dynamic Response of a Supersonic Mixed-Compression Inlet. Paper 68-651, AIAA, June 1968.



POSTMASTER: If Undeliverable (Section 158
Postal Manual) Do Not Return

"The aeronautical and space activities of the United States shall be conducted so as to contribute . . . to the expansion of human knowledge of phenomena in the atmosphere and space. The Administration shall provide for the widest practicable and appropriate dissemination of information concerning its activities and the results thereof."

— NATIONAL AERONAUTICS AND SPACE ACT OF 1958

NASA SCIENTIFIC AND TECHNICAL PUBLICATIONS

TECHNICAL REPORTS: Scientific and technical information considered important, complete, and a lasting contribution to existing knowledge.

TECHNICAL NOTES: Information less broad in scope but nevertheless of importance as a contribution to existing knowledge.

TECHNICAL MEMORANDUMS: Information receiving limited distribution because of preliminary data, security classification, or other reasons.

CONTRACTOR REPORTS: Scientific and technical information generated under a NASA contract or grant and considered an important contribution to existing knowledge.

TECHNICAL TRANSLATIONS: Information published in a foreign language considered to merit NASA distribution in English.

SPECIAL PUBLICATIONS: Information derived from or of value to NASA activities. Publications include conference proceedings, monographs, data compilations, handbooks, sourcebooks, and special bibliographies.

TECHNOLOGY UTILIZATION PUBLICATIONS: Information on technology used by NASA that may be of particular interest in commercial and other non-aerospace applications. Publications include Tech Briefs, Technology Utilization Reports and Notes, and Technology Surveys.

Details on the availability of these publications may be obtained from:

SCIENTIFIC AND TECHNICAL INFORMATION DIVISION
NATIONAL AERONAUTICS AND SPACE ADMINISTRATION
Washington, D.C. 20546